



Evaluation of Cu Back Contact Related Deep Defects in CdTe Solar Cells

P. Kharangarh,^{a,*} D. Misra,^{b,**} G. E. Georgiou,^a and K. K. Chin^a

^aApollo CdTe Solar Energy Center, Department of Physics, New Jersey Institute of Technology (NJIT), University Heights, Newark, New Jersey 07102, USA

^bDepartment of Electrical and Computer Engineering, New Jersey Institute of Technology (NJIT), University Heights, Newark, New Jersey 07102, USA

CdTe solar cells with back contacts formed by either (i) 15nm Cu evaporation followed by application of carbon conductive paste embedded with micron sized Cu particles in ZnTe powder and (ii) only with the above mentioned conducting paste, were evaluated. A Cu-related deep level defect with an activation energy of $E_a \cong 0.57$ eV was observed for Cu evaporated back contact cells and an intrinsic defect with an activation energy $E_a \cong 0.89$ eV was found for cells prepared only by ZnTe:Cu embedded carbon paste. Frequency dispersion in C-V measurements confirms the presence of Cu-related deep level traps for cells with Cu evaporated back contact whereas no such defects were observed in carbon paste contact. The behavior was believed to be due to diffusion of excess Cu from the contact. It was further observed that majority carrier deep level traps (Cu-related or intrinsic) contribute differently to the degradation of electronic properties of the CdTe solar cells.

© 2012 The Electrochemical Society. [DOI: 10.1149/2.001206jss] All rights reserved.

Manuscript submitted July 10, 2012; revised manuscript received August 28, 2012. Published September 20, 2012.

Thin film n⁺-CdS/p-CdTe solar cell research has demonstrated 17.3% efficiency under 1-sun illumination.¹ A stable and non-rectifying back contact is required to maintain the long-term stability of these cells. Electron affinity in CdTe being high, a metal with high enough work function is suitable to form an Ohmic back contact. In the absence of a suitable metal, the back contact behaves like a Schottky barrier in series with the n⁺-CdS/p-CdTe junction diode. Cu-based materials as a back contact have become popular because Cu forms reasonably good Ohmic contacts in p-CdTe.²

However, influence of Cu-based back contacts has been a significant cause of concern as Cu forms deep/semi-shallow defect sites that limits the cell efficiency. Cu related defects can decrease the lifetime, and hence reduced the open circuit voltage (V_{oc}) and fill factor (FF). Studies³⁻⁵ have shown that interstitial Cu impurities can behave as donor but can be converted to acceptors when interacted with Cd vacancies and other Cu ions. Balcioglu et al. studied the Cu-related deep level impurities in polycrystalline CdTe/CdS solar cells.⁶ An anneal step at higher temperatures⁷⁻⁹ is generally used in the back contact formation process for the diffusion and dopant activation. During this step the diffusion of Cu into the CdTe layer is consistent with the reported high diffusion coefficients of Cu in CdTe.^{10,11}

Different techniques are used to find out the Cu-related defects/traps in CdTe.^{9,12-15} Also, the properties of the traps, related to copper, have been extensively studied.¹⁶ Cu is a fast diffuser and it creates substitutional, interstitial and complex defects, so-called AX centers. Different energy levels have been observed by temperature dependent current density versus voltage (J-V-T) characteristics for copper doped CdTe. A more careful study, however, is needed to clarify the contribution of these levels.

In this work, we formed two different sets of Cu-based back contacts by (i) Cu evaporation (excess Cu) and by (ii) Cu doped ZnTe in carbon conductive paste (limited Cu). We have investigated the defects associated with individual contact type by using both temperature dependent J-V and frequency dependent C-V measurements. The J-V results were analyzed based on the Cu diffusion model for the frequency-dependent junction capacitance that is important to understand trap levels if they are near the depletion region of the CdS/CdTe junction. In addition, to elucidate any limitation in solar cell performance, junction capacitance measurements in the CdTe solar cells with excess amount of Cu were performed. The impact of the defects on the solar cell performance, mainly efficiency and fill factor was also evaluated.

Experimental

The n⁺-CdS/p-CdTe solar cell diodes were fabricated with a process similar to that described by Rose et al.¹⁷ The fabrication process, done at NJIT, was explained in detail elsewhere.¹⁸ Two different sets of CdTe solar cells, namely cell¹ and cell² with the areas of 0.25 cm² and 0.56 cm² respectively, were made on 4" × 4" glass substrates at the Apollo CdTe Solar Cell Research Center at NJIT. The only difference in fabrication of devices represented by sets of the cell¹ and the cell² is the variation of back contact process. For sets of cell¹, 15 nm of Cu was directly evaporated using a thermal evaporator on the sample for 20 min. To avoid unwanted heating of and alloying with the sample during evaporation slow deposition process was used to have the required thickness. The deposition rate was found to be approximately 7.5 Å per minute. Slow deposition requires very low base pressure in evaporator so that it does not introduce impurities like O₂ into film. The film thickness was estimated using a time versus thickness curve that was prepared by measuring film thickness after depositing it on bare glass substrates considering the deposition time. Copper evaporation was followed by application of a paste that was prepared by stirring 4 g ZnTe (−140 mesh: Alfa Aesar-44412) with 2 atomic% of Cu, −625 mesh powder (Alfa Aesar- 41205) into 10 g of conducting graphite paste (Acheson Electrodog 114). The paste is thinned as needed with methyl ethyl ketone (MEK) to prepare the samples. For the sets of cell² devices only the above mentioned carbon conductive paste with ZnTe:Cu was applied on the sample. Both the sets of solar cells were annealed at 160°C for 30 minutes.

The J-V characteristics were analyzed in the dark and under 1 sun illumination (~100 mW/cm² for filtered xenon lamp) from the side through the "transparent" glass substrate. Using a Keithley 236 Source Meter temperature dependent J-V-T measurements were carried out. Sample temperature was varied from 25°C to 100°C on a micromanipulator probe station. For frequency-dependent C-V measurements in the dark condition the Agilent HP 4284A impedance analyzer was used.

Results and Discussion

Figure 1 shows the J-V curves under the dark and 1-sun illuminated conditions for sets of cell¹ and cell². Results suggest that open circuit voltage is similar in both the sets of cells but cell² has a large drop in short circuit current density (J_{sc}). This indicates that photocurrent is voltage dependent in cell² due to enhanced leakage, caused possibly by reduction in lifetime of photo-generated carriers. At room temperature, the ideality factor, A in dark condition for sets of cell² (1.9) is higher than sets of cell¹ (1.3) indicating that the diffusion current and recombination current are comparable since typical A value lies

*Electrochemical Society Student Member.

**Electrochemical Society Fellow.

^zE-mail: prk6@njit.edu

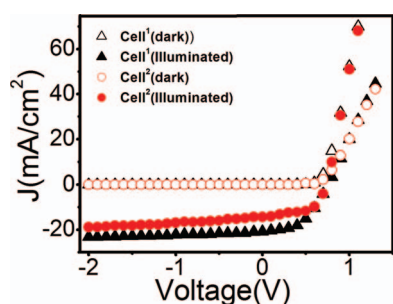


Figure 1. Dark and 1-Sun illuminated J-V curves for both the solar cell types, Cell¹ and Cell².

between 1 and 2.¹⁹ However, recombination current is dominant in sets of cell². Table I outlines all the parameters observed for both the sets of cells. The barrier height was measured in both the sets of cells by using equation in reference.¹⁶ We observed a higher efficiency in cell¹ devices as compared to cell² devices. Presence of varying degree of copper on the back contact has definitely some impact on the quantum efficiency (QE).^{20,21} In our group, work is currently in progress to evaluate its detailed impact on band-gap energy and the results will be published elsewhere.

Generally the J-V relation in heterojunction with Illumination of a generic solar cell with parasitic resistance can be described by any of the diffusion models, either the emission model or the recombination model¹⁹ where the relation is represented by the standard diode equation¹⁹

$$J = J_0 \left[\exp\left(\frac{q(V - R_s J)}{AkT}\right) - 1 \right] - J_L + \frac{(V - R_s J)}{R_{sh}} \quad [1]$$

where q is the electronic charge, A is the effective ideality factor which includes recombination-generation and collection efficiency, T is the absolute temperature, J_0 is an effective reverse saturation current density, V is applied voltage, R_s is the series resistance, k is Boltzmann constant R_{sh} is the shunt resistance and J_L is light current density. R_s

was calculated using the general formula $R_s = \left[\frac{d(\ln(\frac{J}{J_0}))}{dV} \right]^{-1}$ at high forward bias (0.6 to 1.3 V) from the J-V curve and R_{sh} was calculated by using $R_{sh} = \left[\frac{dJ}{dV} \right]_{V=0}^{-1}$ in reverse bias (-1 to -2 V) and included in the Table I. Note that the current is dependent on temperature T .

Analysis of the J-V-T (Reverse bias) at constant voltage yield the following relation to estimate the activation energy

$$E_a = -kT^* \{ \ln(J_0/J_{00}) \} \quad [2]$$

where J_{00} is a constant and E_a is the activation energy. By plotting $\ln(J_0 T^{-2})$ versus $1000/T$ yields a straight line, where the activation energy of the charge carriers, can be estimated from the slope. Figure 2 shows the Arrhenius plot of $\ln(J_0 T^{-2})$ vs. $1000/T$ in the reverse bias at -1 V within the temperature range of 40°C–100°C for each cell. One deep defect/electron-trap was identified in sets of cell¹ with activation

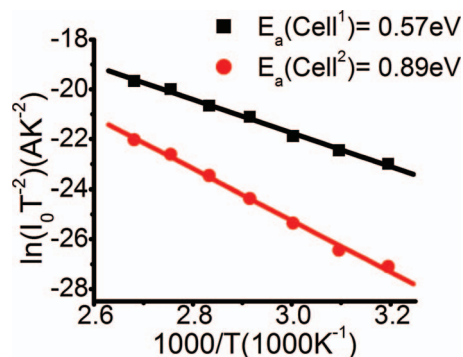


Figure 2. Activation energy of each cell at reverse bias voltage ($V_R = 1V$).

energy of 0.57 eV while deep defect/hole-trap was identified in sets of cell² with activation energy of 0.89 eV respectively.

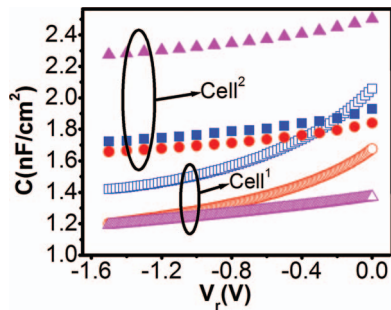
We attempt to identify the nature of traps from their position in the energy gap as determined by the J-V-T measurements. The trap energy level 0.57 eV of sets of cell¹ can be attributed to a deep defect related to copper. This is in good agreement with the activation energy (0.55 eV) for a Cu-related defect obtained from back contact processing, involving Cu and determined using the current-voltage characteristics.²² Also, a deep level trap due to interstitial copper with activation energy of 0.55 eV was observed earlier determined by admittance spectroscopy.²³ It is well known that once the amount of Cu exceeds a threshold level at the back contact it diffuses to the CdTe layer to form Cu related defects either by forming substitutional complexes (Cu_{Cd}^-) or interstitial defects (Cu_i^{2+}). Balcioglu et al.⁶ found through optical deep-level transient spectroscopy (ODLTS) measurements in polycrystalline CdTe/CdS solar cells that the most probable Cu-related defect is a deep donor and may be a doubly ionized Cu interstitial ion (Cu_i^{++}). The observed concentration of the Cu_i^{++} defect corresponded well to the Cu diffusion profile monitored by secondary ion mass spectroscopy (SIMS) with a Cu piled up at the CdTe/CdS interface.^{6,24} It is, therefore, possible that this deep defect level is originated from the Cu-containing back contact due to diffusion of excess Cu that was evaporated. Since sets of cell¹ samples had higher concentration of copper with 15 nm evaporated copper in addition to ZnTe:Cu (2 atomic% Cu) paste, possible formation copper-related defect ($E_V + 0.57$ eV) can be inferred, where E_V is the energy at valence band edge. No such Cu-related defects were observed in sets of cell² samples simply due to the limited availability of Cu at the back contact. Note that sets of cell² only used ZnTe: Cu paste (2 atomic% Cu). The observed energy level of 0.89 eV is believed to be an hole trap. By using photo-induced current transient spectroscopy (PICTS), Rakhshani et al.²⁵ also observed this level, which was identified as the positive Cd_i^{2+} interstitial defect. It is, therefore, reasonable to assume presence of intrinsic defects like Cd_i^{2+} .

To further confirm the presence of Cu in at the CdTe/CdS junction frequency dependent C-V measurements were carried out. A modulation voltage of 5 mV was applied and capacitance was measured within the range of -2 V to 0 V for reverse biased and 0.8 V to 2.0 V for forward biased CdS/CdTe junction. In polycrystalline CdTe solar cells when the applied voltage at the CdS/CdTe junction decreases (reverse bias increases) the depletion region extends toward the back contact. Depending on the thickness of absorber layer the entire CdTe absorber layer can be fully depleted. Because of the large amount of free carriers (10^{23} cm^{-3}) available in the back contact metal, a further increase of reverse bias brings virtually no change in depletion width in the p-CdTe layer. In our case the thickness of the CdTe layer is 12 μm and C-V measurement explores only part of the CdTe thickness from the junction. In addition, the depletion width can be further reduced due to the presence of copper related charge sites from the back contact.

Reverse biased C-V characteristics of sets of cell¹ and cell² in the dark are shown in Fig. 3 at different frequencies. The observed

TABLE I. The relevant parameters of both the cells from Figure 1.

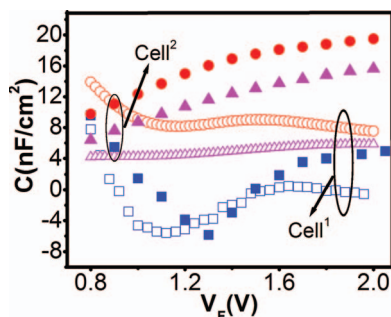
Cells (NJIT)	Cell ¹	Average Values of sets of Cell ¹	Cell ²	Average Values of sets of Cell ²
J_{sc} (mA/cm ²)	20.9	20.2	14.3	14.2
V_{oc} (V)	0.75	0.7	0.75	0.72
FF(%)	54%	51%	55%	51%
η (Eff)(%)	7.7%	7.23%	5.9%	5.2%
A	1.3	1.6	1.9	2.5
J_0 (dark)(mA/cm ²)	3.6×10^{-5}	3×10^{-5}	1.6×10^{-5}	1×10^{-5}
Φ_B (V)	0.52	0.48	0.54	0.50
R_s (Ohm/ cm ²)	0.47	1.73	0.82	2.89
R_{sh} (Ohm/ cm ²)	2.01×10^6	5.77×10^6	2.7×10^5	4.8×10^5



Figures 3. Reverse biased C-V characteristics (-2 V to 0 V) acquired in the dark for sample groups cell¹ (open symbols) and cell² (solid symbols) at frequencies \square \blacksquare 10 KHz, \circ \bullet 100 KHz and \triangle \blacktriangle 1 MHz respectively.

frequency dispersion is opposite in nature for both the sets of cells. The reverse biased capacitance for sets of cell¹ shows that as the frequency increases capacitance reduces significantly below the low frequency level (Fig. 3). For sets of cell², on the other hand, capacitance increases with frequency. The frequency dependence is due to the finite time constant associated with the high concentration defects that are present in the depletion layer.²⁶ In sets of cell¹ when the signal frequency is increased, the reciprocal of emission time constant, the charge variation on the Cu-related deep centers (0.57 eV) in CdTe, cannot follow the signal voltage in the depletion layer and hence cannot contribute to the capacitance.^{27,28} For CdTe, the concentration of deep level defects is comparable to the doping level due to the presence of Cu. In other words, depending on the Cu-related deep electron trap concentration the depletion layer edge was shifted as a function of frequency modifying the depletion layer width. In case of sets of cell², due to the lack of Cu-related defects and the energy level of the observed defect level (0.89 eV) above the intrinsic Fermi level are responsible for the observed reverse effect as shown in Fig. 3.

Fig. 4 shows the forward-biased frequency dispersion of sets of cell¹ and cell² samples in the dark respectively. Assuming a two-diode model as described by Demtsu et al.²⁹ when a forward bias is applied across the device a voltage equivalent to built-in potential is dropped across the CdTe/CdS junction whereas the contact junction becomes reverse biased. According to this assumption, the CdTe thin film solar cell can be split into two depletion regions, the depletion region of the CdTe/CdS junction and a depletion region at back contact barrier region. Under dark condition, when the solar cell is forward biased the back contact junction is reverse biased^{16,30} limiting the current density. So the measured capacitance in forward bias represents mostly the contact junction capacitance.¹⁶ As can be seen in Fig. 4 both the sets of samples have similar frequency dispersion behavior. Higher capacitance was observed for 100 kHz in both cases and once the frequency goes up (1 MHz) capacitance decreased. At 10 kHz there may be strong interference from the junction capacitance¹⁶ in series



Figures 4. Frequency dependent of forward biased (0.8 V to 2.0 V) capacitance measured in the dark at frequencies \square \blacksquare 10 KHz, \circ \bullet 100 KHz and \triangle \blacktriangle 1 MHz for cell¹ (open symbols) and cell² (solid symbols) respectively.

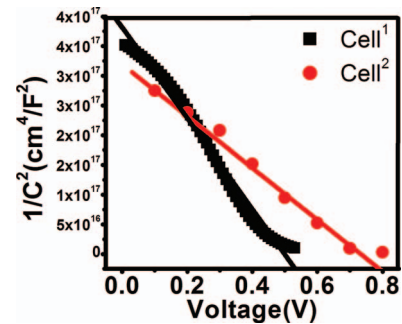


Figure 5. $1/C^2$ versus V curve of each cell in the dark at frequency 100 KHz.

with the contact capacitance showing a minimum in capacitance value in both devices. The time constant of intrinsic defects (~ 10 ms) determines this behavior of frequency dispersion and is similar for both the cases. Only intrinsic traps adjacent to the contact, therefore, contributed to the capacitance, as most of the available Cu had diffused toward the CdTe/CdS junction and piled up in the depletion region. This further confirms our observation in the J-V characteristics and the assumption that defect level in the depletion layer of cell¹ samples is Cu-related.

Figure 5 shows $1/C^2$ versus V curves¹⁹ of two cells in forward bias at 27°C . It is apparent that the variations in back contact processing strongly influences the voltage dependence of the cell capacitance. At reverse bias sets of cell¹ exhibits a larger effective capacitance than sets of cell². However due to the p-CdTe Schottky barrier of the back contact, the measured C is smaller than p-n junction's real capacitance. Therefore, the experimental results from the dark $1/C^2$ versus V curves lead to a hole density for sets of cell¹ = $7 \times 10^{13} \text{ cm}^{-3}$ instead of real acceptor concentration N_a . As we know if the Cu substitutional acceptors are compensated by donor states Cu interstitial Cu_i ; then hole density is lowered which is few order lower than the acceptor concentration, which is consistent with the measured value of hole density in cell¹.³¹ The donor compensation of acceptor is only significant when $p < N_a < N_d$. The hole density for sets of cell² = $3.52 \times 10^{14} \text{ cm}^{-3}$ seems have donor states due to less amount of copper. A high trap density ($N_t = 10^{15} \text{ cm}^{-3}$) of defects resulting for deep donors at the CdS/CdTe junction could also contribute to the reduction in hole density. Contribution of higher amount of Cu in evaporated back contact in sets of cell¹ compared to sets of cell² is further confirmed.

The observed results indicate that presence of an intrinsic defects in the depletion layer significantly degrades the CdTe solar cell performance.³² This was evident in the reduction of efficiency in case of sets of cell². As discussed earlier the recombination current is dominant in sets of cell² indicating the influence of intrinsic defects. Frequency-dependent C-V characteristics also support the presence of majority carrier traps. This clarifies why the efficiency is low in sets of cell². On the other hand even though there is a large concentration of Cu-related deep levels in sets of cell¹ these sites contribute to the hole concentration in the CdTe layer. Since the obtained hole concentration of p-CdTe keeps in the range of 10^{14} – 10^{15} cm^{-3} , instead of desired level of 10^{16} – 10^{17} cm^{-3} , resulting in lower junction band bending and back contact difficulty which contribute to a lower efficiency as compared to the reported value of 17.3% efficiency.

Summary

In summary, we have identified the difference between two different Cu containing back contacts by temperature dependent J-V characteristics. A Cu-related deep level was observed for high Cu containing back contact whereas an intrinsic deep defect level was observed for low Cu containing back contact due to the diffusion of Cu during post-processing annealing. This was further confirmed by the observed frequency dispersion behavior of Cu-related deep level

traps. The performance of device made with evaporated-Cu contact is comparable to that of standard Cu-doped devices.³³ The presence of majority carrier traps (Cu-related or intrinsic) contributes differently to the efficiency and degradation of the electronic properties of the CdTe solar cells.

Acknowledgments

The author gratefully acknowledges the support of the Apollo Solar Energy, based in Chengdu, People's Republic of China. The author specially thanks to Zimeng Cheng and Guogen Liu providing the CdTe Solar cell used in this research. The authors finally thank the members of the NJIT Apollo CdTe Solar Cell research center for processing help and useful discussions.

References

1. K. K. Burger, *First Solar Sets Thin Film CdTe Solar Cell Efficiency World Record*, July 27, 2011.
2. C. R. Corwine, A. O. Pudov, M. Gloeckler, S. H. Demtsu, and J. R. Sites, *Solar Energy Materials & Solar Cells*, **82**(4), 481 (2004).
3. E. Kucys, J. Jerhot, K. Bertulis, and V. Bariss, *Phys. Status Solidi A*, **59**, 91 (1980).
4. B. Monemar, E. Molva, and L. S. Dang, *Phys. Rev. B*, **33**, 1134 (1986).
5. B. Biglari, M. Samimi, M. Hage-Ali, J. M. Koebel, and P. Siffert, *J. Cryst. Growth*, **89**, 428 (1988).
6. A. Balcioglu, R. K. Ahrenkiel, and F. Hasoon, *J. Appl. Phys.*, **88**(12), 7175 (2000).
7. K. K. Chin, T. A. Gessert, and S. H. Wei, *35th IEEE Photovoltaic Proc.*, 1, p. 001915–001918 (2010).
8. S. Demtsu and J. Sites, *IEEE 4th World Conference Photovoltaic Proc.*, p. 523–526 (2006).
9. D. Grecu and A. D. Compaan, *Appl. Phys. Lett.*, **75**(3), 361 (1999).
10. E. D. Jones, N. M. Stewart, and J. B. Mullin, *J. Cryst. Growth*, **117**, 244 (1992).
11. H. H. Woodbury and M. Aven, *J. Appl. Phys.*, **39**, 5485 (1968).
12. F. H. Seymour, V. Kaydanov, and T. R. Ohno, *Appl. Phys. Lett.*, **87**(15), 153507 (2005).
13. K. Zanio, *Cadmium Telluride, Semiconductors and Semimetals*, 13, Academic Press, New York, p. 148 (1978).
14. X. Mathew, *Solar Energy Materials & Solar Cells*, **76**, 225 (2003).
15. S. H. Wei and S. B. Zhang, *Phys. Rev. B*, **66**, 155211 (2002).
16. A. Niemegeers and M. Burgelman, *J. Appl. Phys.*, **81**, 2881 (1997).
17. D. H. Rose, F. S. Hasoon, R. G. Dhere, D. S. Albin, R. M. Ribelin, X. S. Li, Y. Mahathongdy, T. A. Gessert, and P. Sheldon, *Prog. Photovoltaics*, **7**, 331 (1999).
18. P. Kharangarh, D. Misra, G. E. Georgiou, and K. K. Chin, *ECS Transactions*, **41**, 233 (2011).
19. S. M. Sze, *Physics of Semiconductor Devices*, 2nd Edition (Wiley, New York, 1981).
20. S. H. Demtsu, D. S. Albin, J. R. Sites, W. K. Metzger, and A. Duda, *Thin Solid Films*, **516**, 2251 (2008).
21. A. O. Pudov, M. Gloeckler, S. H. Demtsu, J. R. Sites, K. L. Barth, R. A. Enzenroth, and W. S. Sampath, *29th IEEE Photovoltaic Proc.*, p. 760–763 (2002).
22. J. V. Li, S. W. Johnston, X. Li, D. S. Albin, T. A. Gessert, and D. H. Levi, *J. Appl. Phys.*, **108**, 064501 (2010).
23. J. V. Li, R. S. Crandall, I. L. Repins, A. M. Nardes, and D. H. Levi, *37th IEEE Photovoltaic Proc.*, p. 000075–000078 (2011).
24. J. V. Li, J. N. Duenow, D. Kuciauskas, A. Kanevce, R. G. Dhere, Matthew R. Young, and D. H. Levi, *38th IEEE Photovoltaic Proc.*, 1, p. 1–5 (2012).
25. A. E. Rakhshani and Y. Makdasi, *Phys. Status Solidi A*, **179**, 159 (2000).
26. T. A. Gessert, W. K. Metzger, S. E. Asher, M. R. Young, S. Johnston, R. G. Dhere, and A. Duda, *33rd IEEE Photovoltaic Proc.*, p. 1–5 (2008).
27. F. H. Seymore, V. Kaydanov, and T.R. Ohno, *4th IEEE Photovoltaic Proc.*, p. 275–278 (2005).
28. C. T. Sah and V. G. K. Reddi, *IEEE Transactions on Electron Devices*, **11**, 345 (1964).
29. S. H. Demtsu and J. R. Sites, *Thin Solid Films*, **510**, 320 (2006).
30. J. V. Li, A. F. Halverson, O. V. Sulima, S. Bansal, J. M. Burst, T. M. Barnes, T. A. Gessert, and D.H. Levi, *Solar Energy Materials & Solar Cells*, **100**, 126 (2012).
31. K. K. Chin, *Solar Energy Materials & Solar Cells*, **94**(10), 1627 (2010).
32. S. K. Pang, A.W. Smith, and A. Rohatgi, *EEE Transactions on Electron Devices*, **42**, 662 (1995).
33. F. H. Seymour, V. Kaydanov, T. R. Ohno, and D. Albin, *Appl. Phys. Lett.*, **87**, 153507 (2005).